Observation and Measurement of Interaction-Induced Dispersive Optical Nonlinearities in an Ensemble of Cold Rydberg Atoms

Valentina Parigi, Erwan Bimbard, Jovica Stanojevic, Andrew J. Hilliard,*
Florence Nogrette, Rosa Tualle-Brouri, Alexei Ourjoumtsev, and Philippe Grangier
Laboratoire Charles Fabry, Institut d'Optique, CNRS, Université Paris-Sud, 2 Avenue Fresnel, 91127 Palaiseau, France.
(Received 10 September 2012; published 4 December 2012)

We observe and measure dispersive optical nonlinearities in an ensemble of cold Rydberg atoms placed inside an optical cavity. The experimental results are in agreement with a simple model where the optical nonlinearities are due to the progressive appearance of a Rydberg blockaded volume within the medium. The measurements allow a direct estimation of the "blockaded fraction" of atoms within the atomic ensemble.

DOI: 10.1103/PhysRevLett.109.233602 PACS numbers: 42.50.Nn, 03.67.−a, 32.80.Ee, 32.80.Qk

The realization of nonlinear optical effects that are large enough to induce photon-photon interactions would be a significant step forward for quantum information processing and communications. In particular, a strong dispersive and nondissipative nonlinearity could enable the implementation of a two-photon phase gate. It is well known that standard optical nonlinearities, even the largest ones that are typically resonant $\chi^{(3)}$ effects, are too small to reach this range. Presently, two main approaches have been considered to reach the desired regime of deterministic photon-photon interactions. One is cavity (or circuit) quantum electrodynamics (QED), where it is experimentally well established that the atom-field coupling can be large enough to produce single-atom-single-photon interactions [1]. However, in order to use such effects for optical "flying qubits," the challenge is to get very high input-output coupling to the cavity [2]. Another approach is to temporarily convert the photons into strongly interacting particles, for example into dark-state polaritons [3] involving Rydberg atoms. Their interactions lead to a "blockade" phenomenon, where each Rydberg atom blocks the excitation of its neighbors [4,5], which can result in strong nonlinearities [6–9]. Here, we pursue this approach by using an ensemble of cold Rydberg atoms to create large dispersive nonlinearities on a weak "signal" beam. Specifically, we use atoms in a three-level ladder configuration [see Fig. 1(a)] driven by a strong (blue) laser beam, detuned from resonance on the upper transition, and a very weak (red) signal beam on the lower transition. Our scheme is similar to those used in previous work on nonlinearities in three-level systems [10,11]; however, even at optimal performance, the optical nonlinearity produced in those schemes was not large enough to be useful at the single-photon level. Here, the two-photon transition involves Rydberg states in order to exploit their very large van der Waals interactions to further enhance the nonlinearity.

In this Letter, we present the first measurements and a simple physical interpretation of this "giant" dispersive nonlinear effect. At the lowest (nonlinear) order in signal intensity, a $\chi^{(3)}$ behavior is expected, creating intensity-dependent phase shifts. In order to both create and detect

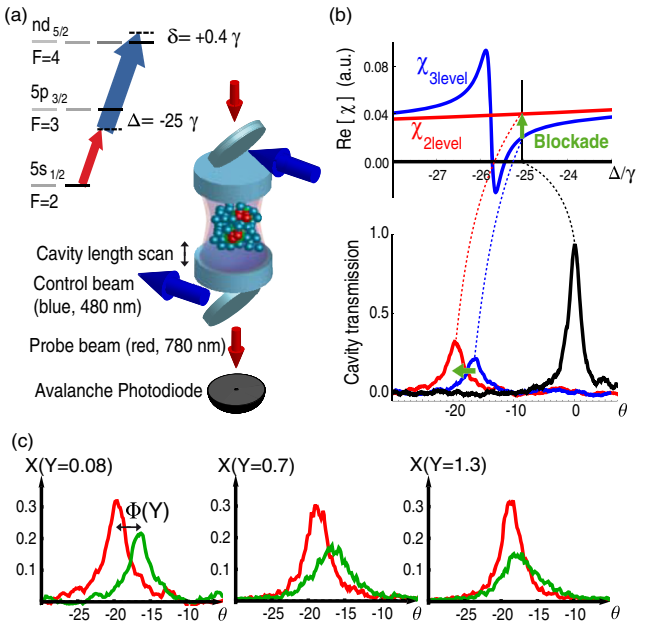

FIG. 1 (color online). (a) An ensemble of N three-level atoms inside an optical cavity is excited by a strong (blue) coupling field, and a weak (red) signal field, all detuned from resonance with respect to the $5S_{1/2} \rightarrow 5P_{3/2} \rightarrow nD_{5/2}$ transitions in Rubidium 87. (b) Principle of the measurements. Lower part: black: cavity scan without atoms, red: without the blue beam, blue: with blue light at very low red intensity. θ is the signal laser-cavity detuning (in units of cavity linewidth), scanned with the cavity length. Upper part: corresponding real part of susceptibilities. The effect of blockade is indicated by the green arrows. (c) Measured transmission versus θ with the coupling field on (green or right) or off (red or left) for different normalized red intensities Y in the case of the $n = 61$ state. The differential peak shift, denoted by $\Phi(Y)$, is reduced by the blockade for increasing intensities (see text).

such phase shifts, we use the following experimental approach. First, in order to increase the dispersive effects with respect to the absorptive ones, the signal and control fields are detuned from all levels [intermediate and Rydberg, see Fig. 1(a)]. Second, the atoms are located inside a low-finesse optical cavity, in order to amplify the effects while keeping a high input-output coupling efficiency. Since the cavity is itself an interferometer, it converts the nonlinear phase shift into a shift of the cavity resonance peak; the position of this peak can be measured as a function of the intensity of the signal light, with and without the coupling blue light.

Theoretically, the system is described by the Hamiltonian for a three-level atomic ensemble in the presence of blue and red laser fields, and the van der Waals interaction potential between Rydberg atoms. This leads to a hierarchy of Bloch equations containing atom-atom correlation operators [12,13]. The susceptibility χ experienced by the signal field is determined by the atomic coherence of the lower transition of the ladder system. As we are interested in its value at low field intensities, the hierarchy may be truncated to second order (two-body correlations), leading to a closed set of equations [12]. The solution of these equations may be performed numerically for the full three-level model, or analytically by appropriate adiabatic eliminations. Both cases recover the result obtained in Ref. [12] for the particular case of zero two-photon detuning.

Additionally, this analysis must take into account that the blue and red light fields have different beam waists, standing wave structures and very different finesses (respectively 2 and 120) in the optical cavity. Hence, the spatial variations of the two fields must be introduced in the numerical evaluation of Bloch equations, and averages performed over the intensity distributions. In addition, the coupling of the injected cavity mode with other transverse cavity modes, induced by the nonlinear term of susceptibility, might produce losses and additional line shifts [14], but this effect was calculated to be negligible in our experimental conditions.

The numerical and analytical solutions we obtained for the dispersive part in the $\chi^{(3)}$ limit confirm a modified version of the "universal scaling" introduced in Ref. [15], where the susceptibility of the medium is expressed as

$$\chi = \chi_{3\text{level}} + p_b(\chi_{2\text{level}} - \chi_{3\text{level}}). \quad (1)$$

Here, $\chi_{2\text{level}}$ is the susceptibility of the lower one-photon transition without blue light, $\chi_{3\text{level}}$ is the susceptibility of the same transition with blue light but without Rydberg-Rydberg interactions, and p_b is the probability for an atom to be blockaded due to the Rydberg-Rydberg interaction. The intuitive explanation of the nonlinear effect is the following: if we inject a very weak red signal beam in the presence of the blue light on the two-photon transition, it will experience the single-atom three-level dispersive phase shift, which corresponds to the blue curve in Fig. 1(b) ($p_b \sim 0$, $\chi \sim \chi_{3\text{level}}$). As the red intensity is increased, the Rydberg state population will increase with the effect that each excited Rydberg atom will detune from the two-photon resonance all neighboring atoms inside a blockade sphere, because of the Rydberg-Rydberg interaction. Therefore, the three-level component of the dispersion will be reduced, and the dispersion of the medium will go back towards its value in absence of blue light, as indicated by the green arrow in Fig. 1(b) ($p_b \to 1$, and thus $\chi \to \chi_{2\text{level}}$). In Eq. (1), $\chi_{2\text{level}}$ and $\chi_{3\text{level}}$ can be obtained from standard 2-level and 3-level optical Bloch equations (without the Rydberg interaction term), while p_b must be inferred from the full model. The result is that, to lowest order in the red beam intensity, one can write the simple relation (holding for a homogeneous system): $p_b = n_b p_3$, where p_3 is the Rydberg population without Rydberg-Rydberg interactions, and n_b is the number of atoms in a blockade sphere [12], more precisely defined by

$$n_b = (2\pi^2/3)\rho\sqrt{|C_6|/\delta_e}. \quad (2)$$

In this expression, ρ is the atomic density, C_6 is the usual coefficient in the van der Waals Rydberg-Rydberg interaction C_6/R^6 [4,5], and δ_e is the two-photon detuning, corrected (and actually increased, see the Appendix) by the blue-induced light shift.

The experimental scheme is shown in Fig. 1(a). A cloud of cold ^{87}Rb atoms in a magneto-optical trap (MOT) is placed into an optical cavity, with finesse $F \sim 120$ and linewidth $\kappa/2\pi \sim 10$ MHz at 780 nm. The atomic sample is cooled to 40 μK by 6 ms of polarization gradient cooling, whereupon the sample is optically pumped to the $5S_{1/2}(F = 2, m_F = 2)$ state. Approximately 1 nW of 780 nm light is coupled into the cavity; the red light is detuned by $\Delta = -75$ MHz $\sim -25\gamma$ below the $5S_{1/2}(F = 2, m_F = 2) \to 5P_{3/2}(F = 3, m_F = 3)$ transition with linewidth γ. The cavity length is scanned around resonance with the red beam. Approximately 100 mW of a 480 nm beam is also injected into the cavity, using a dichroic mirror. The two beams are slightly blue detuned from the two-photon transition toward the Rydberg state $nD_{5/2}(F = 4, m_F = 4)$, with $n = 46$, 50, 56, 61. On the cavity output side, the blue and red beams are separated by a second dichroic mirror, and the 780 nm light is focused on an avalanche photodiode (APD). Since, in order to obtain a strong effect, the two-photon detuning has to be rather small (typically 1 MHz), the locking system of the lasers should be designed to ensure a narrow linewidth of the two-photon transition. For this purpose, the red (780 nm) and blue (480 nm) lasers are locked onto the same "transfer" cavity, as well as a far detuned laser (810 nm) locking the experimental cavity.

The choice of the sign of the detunings is very important, because neither the light shifts nor the Rydberg interactions should bring the atoms (or pairs of atoms) into

resonance, otherwise the losses become very high. This is both predicted theoretically [12] and observed experimentally. We are using $nD_{5/2}$ Rydberg states that have attractive interactions ($C_6 < 0$) and may involve many different potential curves. One reason for this is to fulfill the above condition on the sign of the detunings. The increased risk to create ions in the cloud due to attractive Rydberg-Rydberg interactions is discussed below. The value of $\sqrt{|C_6|}$ is calculated by averaging $\sqrt{|C_6(\lambda)|}$ over potentials U_λ of a given $nD_{5/2} + nD_{5/2}$ manifold, where λ enumerates the molecular states. These effective C_6 lie within 20% from the values calculated in Ref. [16].

The cavity resonance position corresponds to a measured value of $\theta = (\omega - \omega_c)/\kappa$, ω and ω_c being the red laser and cavity frequencies ($\theta = 0$ is the resonance position without atoms). In the absence of blue light and well below one-photon saturation, the atoms induce a shift of this position proportional to $C\chi_{2\text{level}} \sim C\gamma/\Delta$. It depends on the detuning Δ and on the cooperativity parameter $C = Ng^2/2\gamma\kappa$ where g is the usual atom-field coupling parameter, and C takes into account the collective enhancement due to the N atoms within the cavity mode. In the presence of blue light, the shift becomes $\propto C\chi$ where χ is the general susceptibility, expected to be theoretically defined by (1) in our parameter range. We measured the blue-induced part of the resonance shift $\Phi(Y)$ [see Fig. 1(c)], where Y is the red intensity normalized to the saturation intensity at resonance on the lower transition. A significant Y-dependent blue-induced resonance shift at low values of Y is an indication of the desired collisional nonlinear dispersive effect. It is convenient to normalize this shift to its value for vanishing red power, and to consider $\Phi(Y)/\Phi(0)$. From (1) its theoretical value is given by

$$\frac{\Phi(Y)}{\Phi(0)} = \frac{(\chi - \chi_{2\text{level}})}{(\chi_{3\text{level}} - \chi_{2\text{level}})} = 1 - n_b p_3. \qquad (3)$$

To lowest order, $p_3 \propto Y$, so the quantity $1 - n_b p_3$ should manifest a Y dependence and, according to (2), a Rydberg-level dependent behavior. It should be noted that p_3 is also dependent on the blue Rabi frequency (see the Appendix) and, since the different Rydberg levels possess different dipole moments, a given blue power corresponds to different values of Rabi frequency for the different n states. However, after averaging over spatial intensity distributions as discussed above, the averaged $\overline{p_3}$ is only very weakly sensitive to the state-dependent variation of blue Rabi frequency in our parameter range. The principal numbers of the investigated states offer a good compromise between the van der Waals interaction strength (which increases proportionally to n^{11}) and the maximal blue-induced shift which is proportional to the square of the dipole moment and decreases as n^{-3}. The shift is also dependent on the cooperativity which, in the present experiment, is limited to around 200 in order to avoid stronger absorption. Figure 2(a) shows the measured shift versus Y for Rydberg states with different n. Below a certain Y value, the behavior is well described by the function $1 - s_n Y$. As the red power increases, a saturation effect appears: the number of atoms in the Rydberg level stops increasing proportionally to the red intensity. If our simple description is correct, the initial slope s_n should be proportional to $\sqrt{|C_6|}$ which scales as $\sqrt{n^{*11}} = n^{*5.5} = (n-d)^{5.5}$ where $d \approx 1.35$ is the quantum defect [4,5]. However, s_n actually contains an additional contribution from the intrinsic nonlinearity of $\chi_{3\text{level}}$. The measured s_n, corrected for this calculated (small) contribution, are plotted as a function of n^* in log-log scale in Fig. 2(b). A linear fit yields a slope of 6 ± 0.5, consistent with the expected 5.5. To confirm that the observed effect is due to atomic interactions, we show in Fig. 2(c) the results obtained for $n = 61$, by decreasing the atomic density, and keeping the same cooperativity. This is achieved by loading more atoms in the MOT and letting the cloud expand a longer time, so the

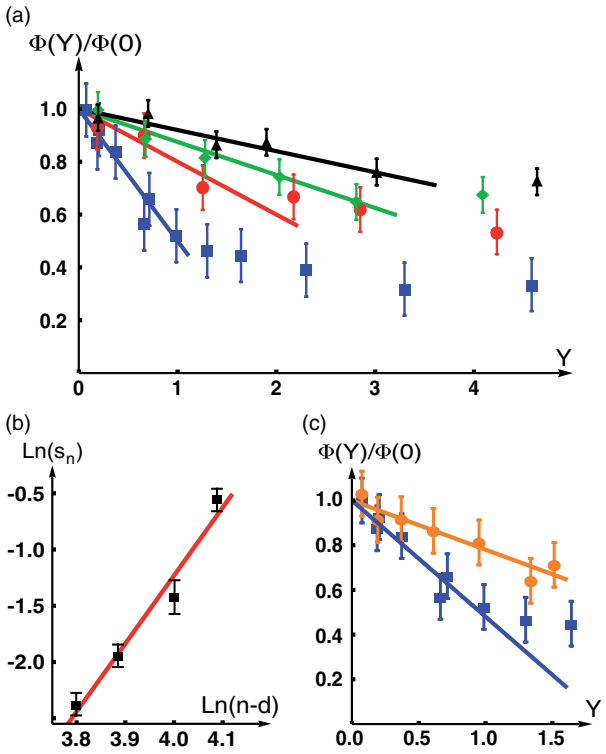

FIG. 2 (color online). (a) Normalized cavity shift $\Phi(Y)/\Phi(0)$ versus normalized input red intensity Y, for several Rydberg states with $n = 46$ (black triangles), 50 (green diamonds), 56 (red circles), 61 (blue squares). The full lines correspond to the initial slopes of the curves, which are expected to be of the form $1 - s_n Y$. (b) Value of s_n as a function of $(n\text{-}d)$, in logarithmic scales. The slope of this curve gives the expected power law behavior. (c) Normalized cavity shift $\Phi(Y)/\Phi(0)$ as a function of the normalized input red intensity Y, for the Rydberg state $n = 61$, for two different atomic densities $\rho_{\text{low}} \sim 0.02$ at/μm^3 (orange circles), and $\rho_{\text{high}} \sim 0.04$ at/μm^3 (blue squares) but for the same number of atoms coupled to the probe mode. The observed change in slope is consistent with the expected ratio $\rho_{\text{high}}/\rho_{\text{low}} \sim 2$ of the densities.

same cooperativity is obtained from a larger cloud with lower density. In that case, one expects a reduced nonlinear collisional effect, since interactions are density dependent (n_b is proportional to ρ). The two sets of data points in the figure correspond to the two values $\rho_{\mathrm{low}} \sim 0.02$ at/μm^3, and $\rho_{\mathrm{high}} \sim 0.04$ at/μm^3: the observed change in slope (by a factor 2.3 ± 0.3) is consistent with the density ratio $\rho_{\mathrm{high}}/\rho_{\mathrm{low}} \sim 2$.

It is also important to take into account the time scale of the experiment. The measurements—the scans of the cavity length around the red resonance—are done in a transient regime: the time it takes to scan one cavity linewidth is approximately 4 μs, which should be compared to the time necessary to reach the steady state value of the Rydberg population. The two times turn out to be of the same order of magnitude, so we have used dynamical rather than steady state solutions, leading to some reduction of the observed nonlinear effect. The final calculated values of the slopes s_n, taking into account spatial averaging and dynamics, agree with the experiment to within 50%.

An additional complication arises from the fact that the blockade effect could be mimicked by the unintended creation of ions in the medium. Such ions can be generated either from single atoms, due to the interaction of Rydberg atoms with the ambient blackbody radiation, or from collisions between Rydberg atoms. In the latter, the collisions are enhanced since we work with Rydberg states with attractive atom-atom potentials. By increasing the laser powers and scanning the cavity at lower speed, we observed typical cascade ion effects [17], which in our case lead to a reduction in the cooperativity through atom loss. However, ions do not seem to play a role in the regime of parameters where we measured $\Phi(Y)/\Phi(0)$. To confirm this, we varied the duration of exposure to the red light during the scans and did not observe significant changes in the nonlinear cavity shift, while the number of ions should change dramatically [17,18]. Furthermore, for the most relevant parameter range, corresponding to the lowest red intensity, the Rydberg state population is actually very small ($< 5\%$), and the number of ions must be even smaller, typically by several orders of magnitude.

In conclusion, it is interesting to compare the observed $\chi^{(3)}$ with other references. The resonance shift we observe for the $n = 61$ Rydberg state corresponds to an effective value of $\mathrm{Re}[\chi^{(3)}] \sim 5 \times 10^{-9}$ m^2/V^2. This value, which is the first measurement of a dispersive nonlinear susceptibility of such magnitude in Rydberg gases, is approximately two orders of magnitude below the value reported in Ref. [19], which was for a stronger absorptive on-resonance process. It is worth noting that in our setup the nonlinear phase shift corresponding to this $\chi^{(3)}$ is multiplied by the cavity finesse.

It can thus be expected that the kind of nonlinearity observed here can be extended to the single-photon regime by reducing the cavity beam waist, increasing the cavity finesse and choosing a Rydberg state with higher quantum number n. Correspondingly, one should increase the blue intensity in order to keep a large enough blue-induced phase shift, despite the decrease of the dipole matrix element as n increases. The linear absorption, dominant in our experiment, can be further reduced by increasing the detunings, but a quantitative description of nonlinear losses requires further investigation. Though much progress is still needed to reach the regime of large dispersive photon-photon interactions in the optical domain, in our system the interaction-induced nonlinearities exceed by several orders of magnitude the usual nonlinearities resulting from a collection of one-atom effects.

This work is supported by the ERC Grant No. 246669 "DELPHI." We thank André Guilbaud and Frédéric Moron for essential help with the experiment.

APPENDIX

We give here explicit expressions of quantities used in the text, obtained from suitable approximations in standard optical Bloch equations. Let us introduce again the number n_b of atoms in a blockade sphere [12], defined by

$$n_b = \frac{2\pi^2\rho}{3}\sqrt{\frac{|C_6|}{\delta - g_b^2/\Delta}}, \tag{4}$$

where C_6 is the standard van der Waals coefficient, δ is the two-photon detuning ($\delta > 0$), Δ the one-photon detuning ($\Delta < 0$), and g_b the blue laser Rabi frequency. To lowest order for our experimental parameters, the Rydberg population p_3 without interactions is

$$p_3 = \frac{g_a^2 g_b^2}{\Delta^2(\delta - g_b^2/\Delta)^2}\frac{(\gamma_b\Delta^2 + \gamma g_b^2)}{(\gamma_c\Delta^2 + \gamma g_b^2)}, \tag{5}$$

where g_a is the red Rabi frequency ($Y \propto g_a^2$), γ_b and γ_c are the coherence and population damping rates of the Rydberg level. The real part of the "differential" susceptibility is

$$(\chi_{3\mathrm{level}} - \chi_{2\mathrm{level}}) \propto \frac{g_b^2}{\Delta^2(\delta - g_b^2/\Delta)}. \tag{6}$$

As noted above, averaging over the spatial distributions of intensities has been carried out for comparison with the experimental data.

*Present address: QUANTOP, Institut for Fysik og Astronomi, Aarhus Universitet, Ny Munkegade 120, 8000 Aarhus C, Denmark.

[1] S. Haroche and J.-M. Raimond, *Exploring the Quantum: Atoms, Cavities, and Photons* (Oxford University Press, Oxford, 2006).

[2] K. M. Birnbaum, A. Boca, R. Miller, A. D. Boozer, T. E. Northup, and H. J. Kimble, Nature (London) **436**, 87 (2005).

[3] M. Fleischhauer, A. Imamoglu, and J. P. Marangos, Rev. Mod. Phys. **77**, 633 (2005).
[4] M. Saffman, T. G. Walker, and K. Moelmer, Rev. Mod. Phys. **82**, 2313 (2010).
[5] D. Comparat and P. Pillet, J. Opt. Soc. Am. B **27**, A208 (2010).
[6] J. D. Pritchard, D. Maxwell, A. Gauguet, K. J. Weatherill, M. P. A. Jones, and C. S. Adams, Phys. Rev. Lett. **105**, 193603 (2010).
[7] Y. O. Dudin and A. Kuzmich, Science **336**, 887 (2012).
[8] T. Peyronel, O. Firstenberg, Q.-Y. Liang, S. Hofferberth, A. V. Gorshkov, T. Pohl, M. D. Lukin, and V. Vuletić, Nature (London) **488**, 57 (2012).
[9] D. Maxwell, D. J. Szwer, D. P. Barato, H. Busche, J. D. Pritchard, A. Gauguet, K. J. Weatherill, M. P. A. Jones, and C. S. Adams, arXiv:1207.6007.
[10] K. M. Gheri, P. Grangier, J.-P. Poizat, and D. F. Walls, Phys. Rev. A **46**, 4276 (1992).
[11] J.-F. Roch, K. Vigneron, P. Grelu, A. Sinatra, J.-P. Poizat, and P. Grangier, Phys. Rev. Lett. **78**, 634 (1997).
[12] S. Sevinçli, N. Henkel, C. Ates, and T. Pohl, Phys. Rev. Lett. **107**, 153001 (2011).
[13] J. Stanojevic and R. Côté, Phys. Rev. A **81**, 053406 (2010).
[14] J.-M. Courty and A. Lambrecht, Phys. Rev. A **54**, 5243 (1996).
[15] C. Ates, S. Sevinçli, and T. Pohl, Phys. Rev. A **83**, 041802 (2011).
[16] A. Reinhard, T. C. Liebisch, B. Knuffman, and G. Raithel, Phys. Rev. A **75**, 032712 (2007).
[17] M. Viteau, A. Chotia, D. Comparat, D. A. Tate, T. F. Gallagher, and P. Pillet, Phys. Rev. A **78**, 040704 (2008).
[18] F. Robicheaux, J. Phys. B **38**, S333 (2005).
[19] J. D. Pritchard, A. Gauguet, K. J. Weatherill, and C. S. Adams, J. Phys. B **44**, 184019 (2011).